Structural Engineering and Mechanics, Vol. 6, No. 7 (1998) 757-772
DOI: http://dx.doi.org/10.12989/sem.1998.6.7.757

Progressive failure of symmetric laminates under in-plane shear: II-Negative shear

S.B. Singh†, Ashwini Kumar‡ and N.G.R. Iyengar‡†

Indian Institute of Technology Kanpur, Kanpur 208016, India

Abstract. The objective of the present work is to estimate the strength and failure characteristics of symmetric thin square laminates under negative shear load. Two progressive failure analyses, one using the Hashin criterion and the other using a Tensor polynomial criterion, are used in conjunction with the finite element method. First-order shear-deformation theory along with geometric nonlinearity in the von Karman sense has been incorporated in the finite element modeling. Failure loads, associated maximum transverse displacements, locations and modes of failure including the onset of delamination are discussed in detail; these are found to be quite different from those for the positive shear load reported in Part I of this study (Singh *et al.* 1998).

Key words: progressive failure; laminated plate; failure criteria; in-plane negative shear.

1. Introduction

It is well known that the total failure of a laminated composite panel does not always occur at the load corresponding to the first-ply failure. Moreover, failure characteristics of heterogeneous and anisotropic laminates are completely different from those of isotropic ones. Further, responses of anisotropic laminates under positive and negative directions of the shear load are also different (Kosteletos 1992, Zhang & Matthews 1984). Thus, the knowledge of strength and failure characteristics of laminated plates under in-plane shear loads (positive and negative) is essential so that designers can fully exploit postbuckled reserve strength of laminates in the design of composite structural panels. Early investigations related to the failure of laminated plates under uni-axial compression are by Engelstad *et al.* (1992) and Lee & Hyer (1993). Very recently, Singh *et al.* (1997, 1998) have presented progressive failure results for symmetric laminates subjected to uni-axial compression and positive in-plane shear load, respectively, using various failure criteria.

The present study is, infact, the extension of the work of Singh *et al.* (1998) for the case of in-plane negative shear load. It deals with the investigation of failure loads and failure characteristics of thin, square and symmetric laminates with five different lay-ups. The boundary conditions are the same as for the positive shear load (Singh *et al.* 1998) and are shown in Fig. 1 for the sake of convenient reference. Two progressive failure procedures are

† Presently, Lecturer, Department of Applied Mechanics, M.N.R.E.C. Allahabad
‡ Professor, Department of Civil Engineering
‡† Professor, Department of Aerospace Engineering

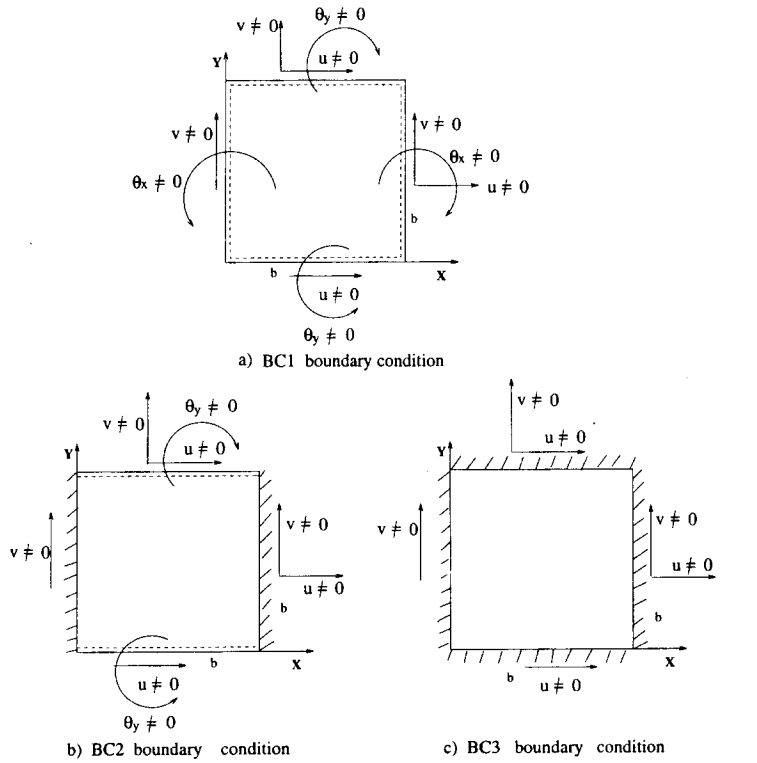

Fig. 1 Details of various boundary conditions for full plate

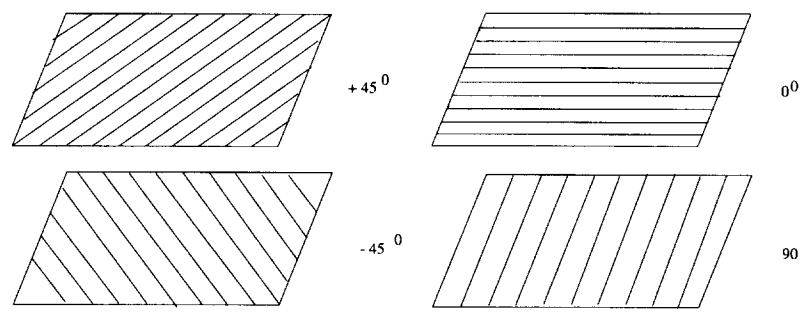

Fig. 2 Schematics of ply orientation in laminate A

used, one with the Hashin (1980) failure criterion and the other with the tensor polynomial forms of the maximum stress, maximum strain, Tsai-Hill, Hoffman and Tsai-Wu criteria. The material property degradation model used with the Hashin criterion is based on Tsai (1986) and that with Tensor Polynomial Criteria is based on Engelstad *et al.* (1992).

2. Methodology

A special-purpose computer program was developed to carry out the present study which is based on the finite element formulation using the first-order shear-deformation theory with a

Table 1 Lamination schemes of symmetric laminates

Lamination scheme	*$(\pm 45/0/90)_{2s}$	$(\pm 45/0_2)_{2s}$	$(\pm 45)_{4s}$	$(\pm 45/0_6)_s$	$(0/90)_{4s}$
Type	A	B	C	D	E

*The terms within the parenthesis are fiber orientations of the ply-group (see Fig. 2 for the ply orientation of the basic ply-group of laminate A) and the digit in the subscript represents the repetition of the ply-group on one side of the mid-plane of the laminate whiles represents the symmetry of the laminate about the mid-plane.

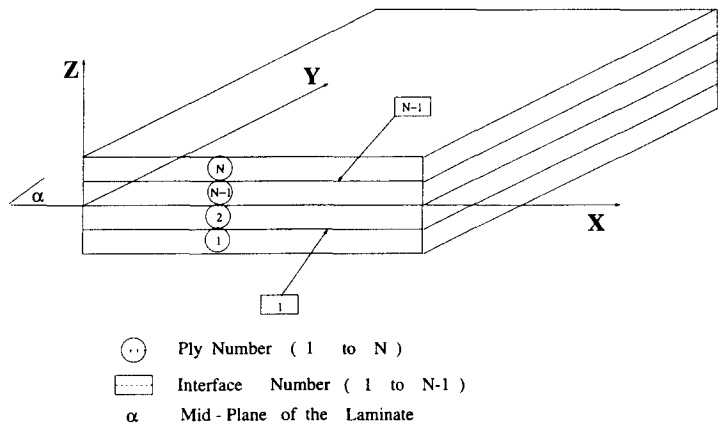

Fig. 3 Ply and interface numbering within the laminate

nine noded Lagrangian element having five degrees of freedom per node. Geometric nonlinearity based on von Karman's assumptions was incorporated. The nonlinear algebraic equations are solved using the Newton-Raphson technique. The calculation of stresses is done on the nodal points. Due to connectivity of a particular node to various elements, nodal point stresses are calculated taking the average value of stresses at that node from various elements associated with that node. All the six stress components are calculated at each nodal point. However, to predict the failure of a lamina, only five stress components (three in-plane stress and two transverse shear stress) are used in the selected failure criterion. To predict the onset of delamination, transverse stresses (two shear stress components and one normal stress component) are used in the maximum stress failure criterion. Delamination at any interface is said to occur when any of the transverse stress components in any of the two layers adjacent to interface becomes equal to or greater than its corresponding strength. The ply failure is said to occur when the state of stress at any point within the lamina satisfies the selected failure criterion. The first-ply failure refers to the situation at which one or more than one plies fail first as the load is increased. After the first-ply failure, the progressive failure analysis is carried out using progressive failure procedure appropriate to the selected failure criterion. Details of various failure criteria and progressive failure procedures employed in the present work are presented in Part-I (Singh *et al.* 1998) of this study; for the sake of brevity these are omitted here.

A total of five symmetric lamination schemes are employed to investigate the progressive failure. Individual laminates are designated from A to E for identification. The details of the lamination schemes are shown in Table 1. The ply and the interface numbering scheme

Table 2 Material properties of T300/5208 (Pre-peg)$^{\oplus}$ graphite-epoxy

Mechanical properties	Values	Strength properties	Values
E_1	132.58 Gpa	X_t	1.515 Gpa
E_2	10.8 Gpa	X_c	1.697 Gpa
E_3	10.8 Gpa	$Y_t=Z_t$	43.8 Mpa
$G_{12}=G_{13}$	5.7 Gpa	$Y_c=Z_c$	43.8 Mpa
$\nu_{12}=\nu_{13}$	0.24	R	67.6 Mpa
ν_{23}	0.49	$S=T$	86.9 Mpa

$\oplus$ Pre-peg refers to the graphite fibers impregnated with epoxy resin and available in tape form.

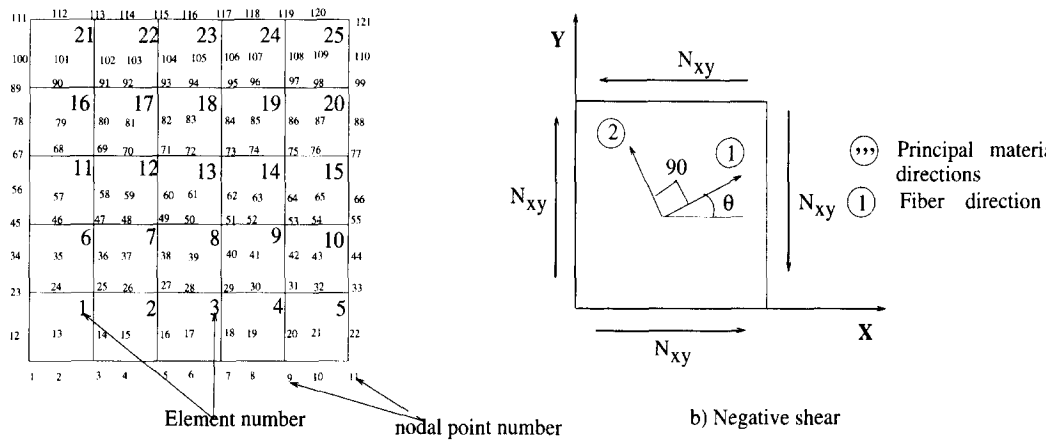

Fig. 4 Finite element mesh for full plate and the sign convention for applied shear load

within the laminate is shown in Fig. 3. Properties of the material of the laminate (Reddy and Reddy 1992) are presented in Table 2.

In the Table E_1, E_2, E_3 are the principal Young's moduli while G_{12}, G_{13}, G_{23} are the shear moduli corresponding to the planes 1-2, 1-3, and 2-3 respectively and, ν_{12}, ν_{13}, ν_{23} are the corresponding Poisson's ratios. In this study a full square plate of width b is used with 25 element mesh, the details of which are shown in Fig. 4(a). Three types of flexural boundary conditions, namely BC1, BC2, BC3, have been considered; BC1- refers to a plate with all edges simply supported, BC2- refers to a plate with two longitudinal edges (y=0 and y=b) simply supported and the other two edges clamped and BC3- refers to a plate with all edges clamped. In all the three cases the in-plane boundary conditions (Fig. 1) are identical and the shear load is applied on all the four edges as shown in Fig. 4b. Results for failure loads and corresponding displacements are presented in the following nondimensionalized forms:

In-plane shear load=$N_{xy}b^2/E_2h^3$

Maximum transverse displacement=w_{max}/h

where h is the total thickness of the laminate and N_{xy} is the applied in-plane shear load per unit length.

Table 3a Progressive failure results for $(\pm 45/0/90)_{2s}$ laminate with BC1 boundary condition

Failure criteria	First-ply failure load	Ultimate failure load	$(w_{max}/h)^{\oplus}$	*FL*†	*FP*‡	Mode of first-ply failure
Maximum stress	83.05 (7.2)*	128.66 (2.4)	2.43	1	2	Transverse
Maximum strain	74.01 (−4.4)	75.73 (−40.3)	2.03	2	111	Transverse
Tsai-Hill	83.05 (7.2)	126.94 (1.0)	2.43	1	11	Transverse
Tsai-Wu	77.45 (0.0)	125.65 (0.0)	2.19	2	11	Transverse
Hoffman	83.05 (7.23)	125.65 (0.0)	2.43	1	11	Transverse
Hashin	77.45 (0.0)	107.58 (14.38)	2.19	4	1	Tensile matrix

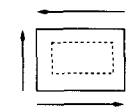

⊕ Non-dimensionalized maximum transverse displacement in the plate at the first-ply failure

† First failed layer number; ‡ First failed nodal point number

*Percentage difference based on Tsai-Wu criterion

Table 3b Progressive failure results of $(\pm 45/0_2)_{2s}$ laminate with BC1 boundary condition

Failure criteria	First-ply failure load	Ultimate failure load	$(w_{max}/h)^{\oplus}$	*FL*†	*FP*‡	Mode of first-ply
Maximum stress	74.87 (4.2)*	97.68 (−0.44)	2.36	2	21	Transverse
Maximum strain	68.85 (−4.2)	89.07 (−9.2)	2.03	2	11	Transverse
Tsai-Hill	74.87 (4.2)	98.11 (0.0)	2.36	2	21	Transverse
Tsai-Wu	71.86 (0.0)	98.11 (0.0)	2.20	2	11	Transverse
Hoffman	74.87 (4.2)	96.82 (−1.3)	2.36	2	21	Transverse
Hashin	69.71 (−3.0)	93.80 (−4.4)	2.08	2	21	Compressive matrix

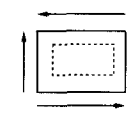

⊕ Non-dimensionalized maximum transverse displacement in the plate at the first-ply failure

† First failed layer number; ‡ First failed nodal point number

*Percentage difference based on Tsai-Wu criterion

3. Results and discussion

3.1. Laminates with BC1 boundary condition

Progressive failure results are presented in Tables 3a-3e. To have the idea of variations in failure loads predicted by various failure criteria, the maximum percentage difference in first-ply failure loads predicted by failure criteria for all five lay-ups (A, B, C, D and E) is shown

Table 3c Progressive failure results of $(\pm 45)_{4s}$ laminate with BC1 boundary condition

Failure criteria	First-ply failure load	Ultimate failure load	$(w_{max}/h)^{\oplus}$	*FL*†	*FP*‡	Mode of first-ply failure
Maximum stress	86.49 (4.7)*	102.41 (1.3)	3.13	1	11	Transverse
Maximum strain	80.46 (−2.6)	101.98 (0.85)	2.75	1	11	Transverse
Tsai-Hill	86.06 (4.2)	100.69 (−0.43)	3.10	1	11	Transverse
Tsai-Wu	82.62 (0.0)	101.12 (0.0)	2.89	1	1	Transverse
Hoffman	86.06 (4.2)	101.12 (0.0)	3.10	1	1	Transverse
Hashin°	58.20 (−29.6)	89.07 (−11.9)	3.05	1	111	Tensile matrix

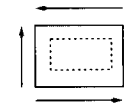

⊕ Non-dimensionalized maximum transverse displacement in the plate at the first-ply failure
† First failed layer number; ‡ First failed nodal point number
*Percentage difference based on Tsai-Wu criterion

Table 3d Progressive failure results of $(\pm 45/0_6)_s$ laminate with BC1 boundary condition

Failure criteria	First-ply failure load	Ultimate failure load	$(w_{max}/h)^{\oplus}$	*FL*†	*FP*‡	Mode of first-ply failure
Maximum stress	49.06 (−5.8)*	80.03 (0.0)	0.95	3	1	Transverse
Maximum strain	45.18 (−13.2)	71.86 (−10.2)	0.38	3	1	Transverse
Tsai-Hill	49.50 (−5.0)	80.03 (0.0)	1.0	3	1	Transverse
Tsai-Wu	52.07 (0.0)	80.03 (0.0)	1.24	3	1	Transverse
Hoffman	49.05 (−5.8)	80.03 (0.0)	0.95	3	1	Transverse
Hashin	44.32 (−14.9)	74.01 (−7.5)	0.12	3	1	Tensile matrix

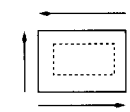

⊕ Non-dimensionalized maximum transverse displacement in the plate at the first-ply failure
† First failed layer number; ‡ First failed nodal point number
*Percentage difference based on Tsai-Wu criterion

in Fig. 5 by means of a histogram for both the positive and negative shear load cases. Coloured bars represent the values for the positive shear load (Singh *et al.* 1998). The corresponding histogram for maximum percentage difference in ultimate failure loads is shown in Fig. 6. It is observed that the first-ply failure locations are identical for laminates D and E, while these are different for laminates A, B and C. Locations of failed points are found to be near the corner for almost all the laminates. It is also observed (although not shown in figures and tables) that in all laminates the progressive failure initiates primarily

Table 3e Progressive failure results of $(0/90)_{4s}$ laminate with BC1 boundary condition

Failure criteria	First-ply failure load	Ultimate failure load	$(w_{max}/h)^{\oplus}$	*FL*†	*FP*‡	Mode of first-ply failure
Maximum stress	45.61 (−14.5)*	58.95 (0.0)	1.24	1	1	Transverse
Maximum strain	43.46 (−18.6)	58.09 (−1.5)	1.07	1	1	Transverse
Tsai-Hill	46.47 (−12.9)	58.52 (−0.73)	1.30	1	1	Transverse
Tsai-Wu	53.36 (0.0)	58.95 (0.0)	1.72	1	1	Transverse
Hoffman	46.04 (−13.7)	58.952 (0.0)	1.28	1	1	Transverse
Hashin	32.70 (−38.7)	36.15 (−38.7)	(0.0°)	1	1	Tensile matrix

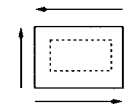

⊕ Non-dimensionalized maximum transverse displacement in the plate at the first-ply failure
† First failed layer number; ‡ First failed nodal point number
*Percentage difference based on Tsai-Wu criterion
° First-ply failure occurs before the buckling load

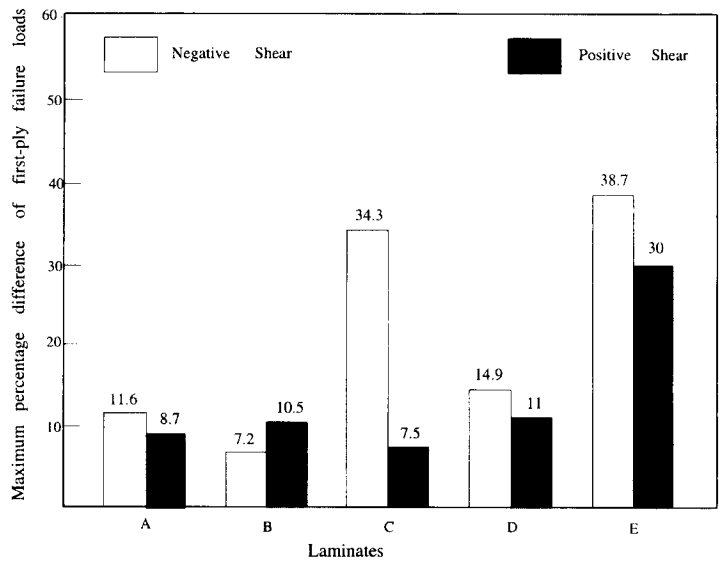

Fig. 5 Histogram showing maximum percentage difference in first-ply failure loads predicted by failure criteria

owing to in-plane normal stresses at right angles to the fiber direction; then an in-plane shear mode of failure occurs in the case of laminates *A*, *B* and *E*; while the fibers fail in the case of laminate *D* and a widespread in-plane shear mode of failure occurs in the case of laminate *C*. It is worth noting (although not shown in tables) that fibers fail in laminates *A* and *B* at a load closer to the ultimate load, while widespread in-plane shear mode of failure eventually leads to the collapse in laminate *C* and fiber failure followed by transverse shear mode of

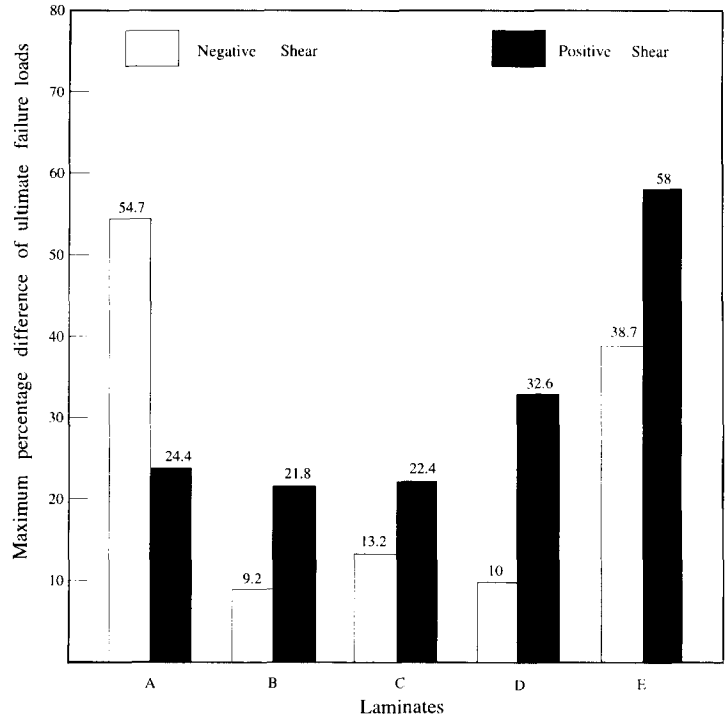

Fig. 6 Histogram showing maximum percentage difference in ultimate failure loads predicted by failure criteria

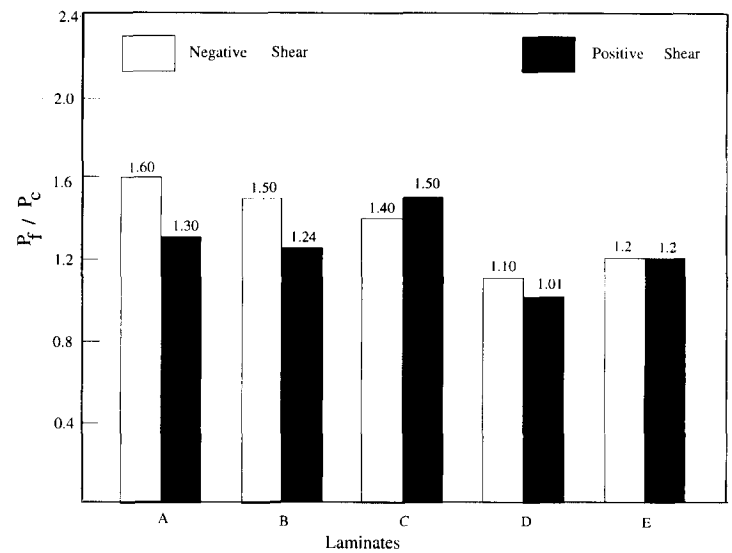

Fig. 7 Histogram showing ratio of the average first-ply failure loads and buckling load of laminates for BC1 boundary condition

failure lead to delaminations in laminate D at all interfaces along the edge y=0. In order to have the estimate of strength beyond buckling, the ratio of first-ply failure load (P_f) and

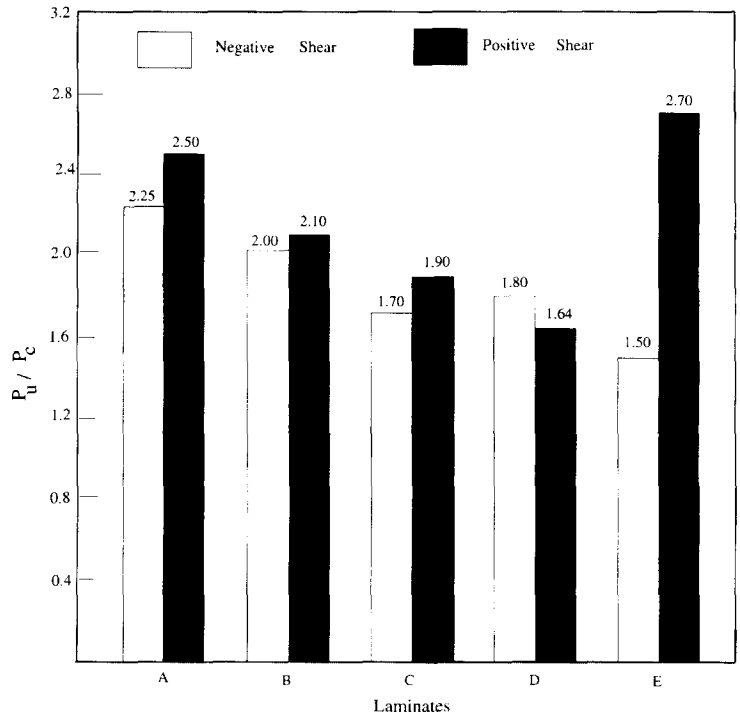

Fig. 8 Histogram showing ratio of the average ultimate failure loads and buckling load of laminates for BC1 boundary condition

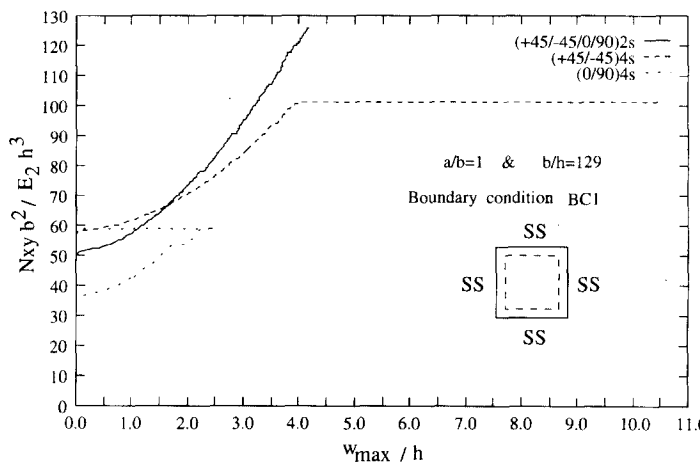

Fig. 9 Progressive failure response using Tsai-Wu criterion for different lay-ups with BC1 boundary condition

buckling load (P_c) for all the five lay-ups is shown by means of a histogram (see Fig. 7), while the corresponding histogram showing ratio of ultimate failure load (P_u) and buckling load (P_c) is shown in Fig. 8. The progressive failure responses for three typical laminates are shown in Figs. 9 and 10 using the Tsai-Wu criterion and the Hashin criteria respectively. It is

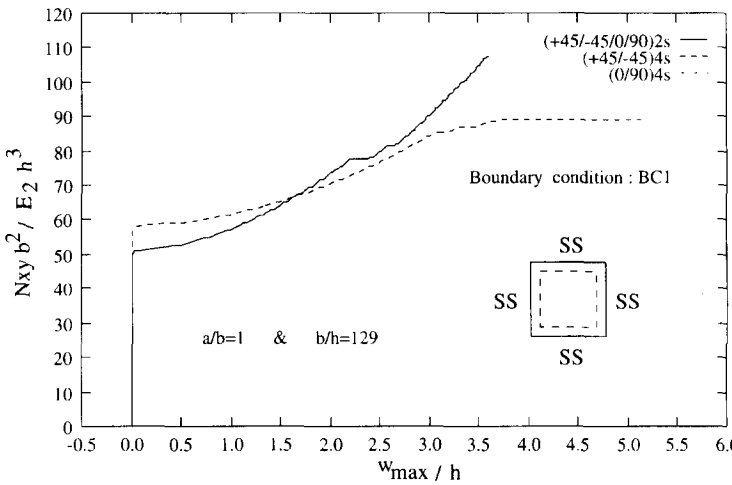

Fig. 10 Progressive failure response using Hashin criterion for different lay-ups with BC1 boundary condition

worth noting that for laminate E, no transverse deflection is observed till its total failure in the case of the Hashin criterion; the reason is that the first-ply failure occurs before the onset of buckling. The absolute maximum value of the (w_{max}/h) obtained for various failure criteria under this loading is found to occur in laminate C and is equal to 4.95 while the corresponding value for the positive shear is 4.39 and is for laminate B (Singh *et al.* 1998).

3.2. $(\pm 45/0/90)_{2s}$ laminate with different boundary conditions

Progressive failure results of this laminate for three different boundary conditions are

Table 4a Progressive failure results of $(\pm 45/0/90)_{2s}$ laminate with BC1 boundary condition

Failure criteria	First-ply failure load	Ultimate failure load	$(w_{max}/h)^{\oplus}$	*FL*†	*FP*‡	Mode of first-ply failure
Maximum stress	83.05 (7.2)*	128.66 (2.4)	2.43	1	2	Transverse
Maximum strain	74.01 (−4.4)	75.73 (−40.3)	2.01	2	111	Transverse
Tsai-Hill	83.05 (7.2)	126.94 (1.0)	2.43	1	11	Transverse
Tsai-Wu	77.45 (0.0)	125.65 (0.0)	2.19	2	11	Transverse
Hoffman	83.05 (7.2)	125.65 (0.0)	2.43	1	11	Transverse
Hashin	77.45 (0.0)	107.58 (14.4)	2.19	4	1	Tensile matrix

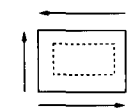

$^{\oplus}$ Non-dimensionalized maximum transverse displacement in the plate at the first-ply failure
† First failed layer number; ‡ First failed nodal point number
*Percentage difference based on Tsai-Wu criterion

Table 4b Progressive failure results of $(\pm 45/0/90)_{2s}$ laminate with BC2 boundary condition

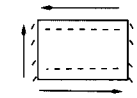

Failure criteria	First-ply failure load	Ultimate failure load	$(w_{max}/h)^{\oplus}$	$FL\dagger$	$FP\ddagger$	Mode of first-ply failure
Maximum stress	93.8 (2.4)*	101.12 (4.0)	1.50	14	33	Transverse
Maximum strain	89.93 (−1.9)	95.96 (−1.3)	1.31	15	33	Transverse
Tsai-Hill	91.65 (0.0)	97.25 (0.0)	1.40	15	33	Transverse
Tsai-Wu	91.65 (0.0)	97.25 (0.0)	1.40	15	33	Transverse
Hoffman	91.65 (0.0)	97.25 (0.0)	1.40	15	33	Transverse
Hashin	74.87 (−18.3)	128.23 (31.86)	0.0◓	4	1	Tensile matrix

$^{\oplus}$ Non-dimensionalized maximum transverse displacement in the plate at the first-ply failure

† First failed layer number; ‡ First failed nodal point number

*Percentage difference based on Tsai-Wu criterion

◓ First-ply failure occurs before buckling of the laminate

Table 4c Progressive failure results of $(\pm 45/0/90)_{2s}$ laminate with BC3 boundary condition

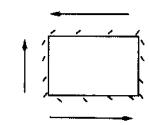

Failure criteria	First-ply failure load	Ultimate failure load	$(w_{max}/h)^{\oplus}$	$FL\dagger$	$FP\ddagger$	Mode of first-ply failure
Maximum stress	103.30 (−6.3)*	114.89 (0.37)	0.91	1	1	Transverse
Maximum strain	98.54 (−10.60	110.16 (−3.8)	0.62	1	1	Transverse
Tsai-Hill	105.0 (−4.7)	110.16 (−3.8)	1.01	1	1	Transverse
Tsai-Wu	110.16 (0.0)	114.46 (0.0)	1.32	1	1	Transverse
Hoffman	103.70 (−5.9)	110.16 (−3.8)	0.94	1	1	Transverse
Hashin	74.87 (−32.0)	124.35 (12.4)	0.0◓	1	1	Tensile matrix

$^{\oplus}$ Non-dimensionalized maximum transverse displacement in the plate at the first-ply failure

† First failed layer number; ‡ First failed nodal point number

*Percentage difference based on Tsai-Wu criterion

◓ First-ply failure occurs before buckling of the laminate

presented in Tables 4a-4c. In order to see the variation of failure loads of this laminate with different boundary conditions (BC1, BC2 and BC3), the maximum percentage difference in first-ply failure loads predicted by various failure criteria is shown in the histogram (see Fig.

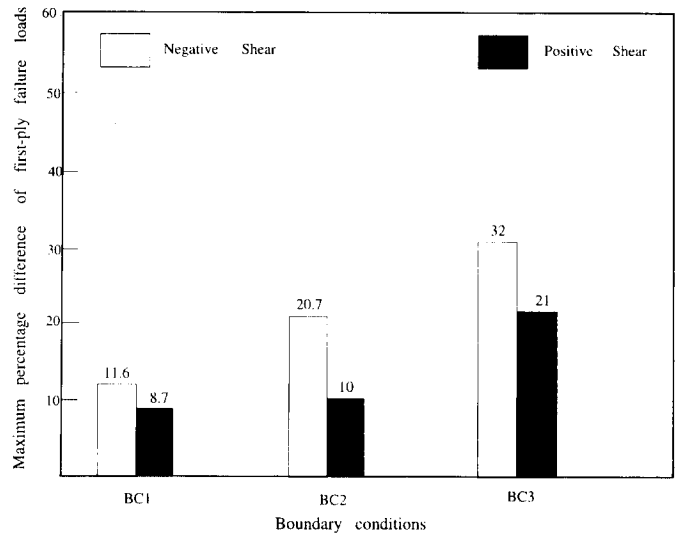

Fig. 11 Histogram showing maximum percentage difference in first-ply failure loads predicted by failure criteria for $(\pm 45/0/90)_{2s}$ laminate with different boundary conditions

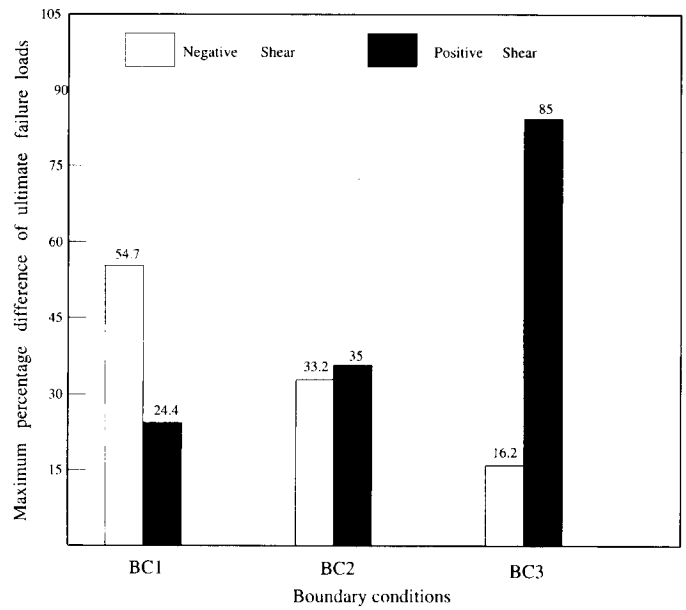

Fig. 12 Histogram showing maximum percentage difference in ultimate failure loads predicted by failure criteria for $(\pm 45/0/90)_{2s}$ laminate with different boundary conditions

11) and the corresponding histogram for ultimate failure load is shown in Fig. 12. Further, to have the estimate of failure loads of this laminate beyond buckling, the ratio of the average value of first-ply failure loads and the buckling load for boundary conditions (BC1, BC2 and BC3) is shown in the histogram (see Fig. 13). The corresponding histogram showing ratio of average ultimate failure load to the buckling load is presented in Fig. 14. It is worth noting

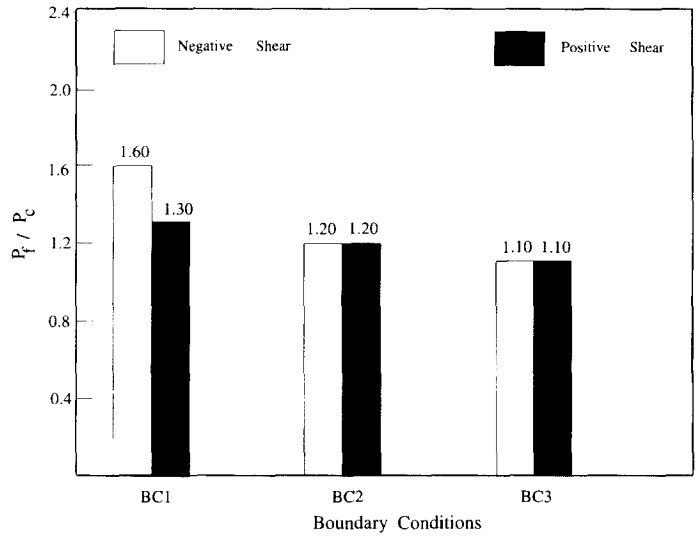

Fig. 13 Histogram showing ratio of the average first-ply failure loads and buckling load of $(\pm 45/0/90)_{2s}$ laminate with different boundary conditions

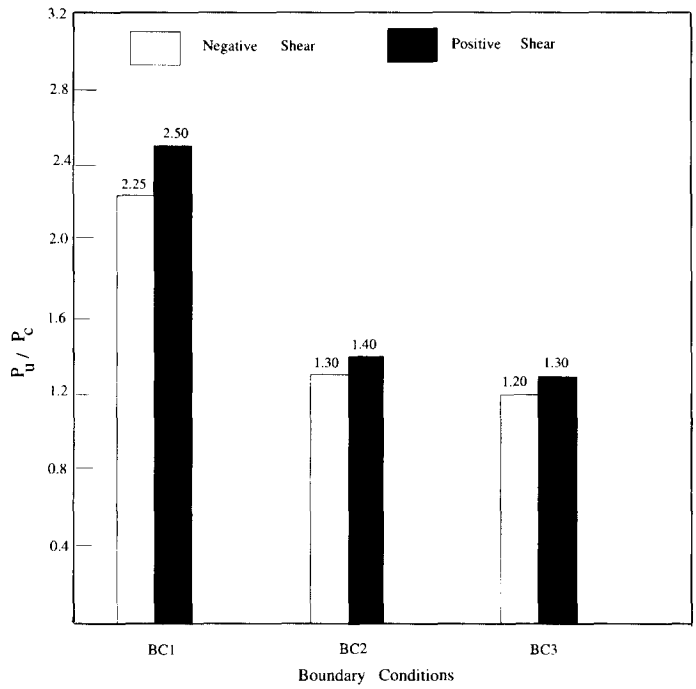

Fig. 14 Histogram showing ratio of the average ultimate failure loads and buckling load of $(\pm 45/0/90)_{2s}$ laminate with different boundary conditions

that the ultimate failure for BC1 boundary condition usually occurs after the fiber failure. However, in the case of BC2 and BC3 the onset of delamination precedes the fiber breakage. The progressive failure response has been shown graphically in Figs. 15 and 16 using the

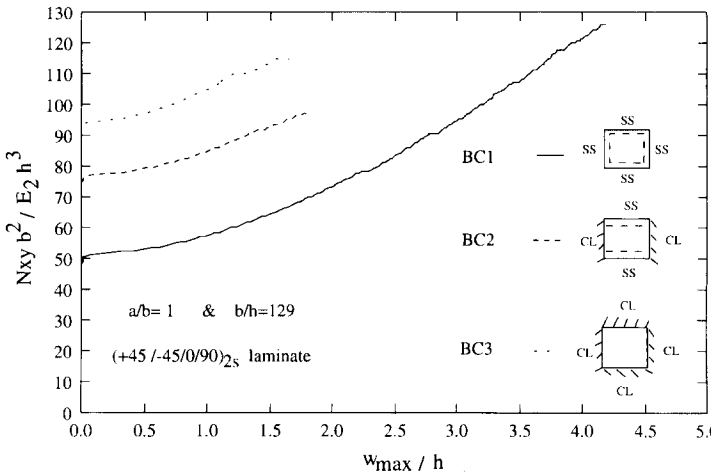

Fig. 15 Progressive failure response of $(\pm 45/0/90)_{2s}$ quasi-isotropic laminate with Tsai-Wu criterion for different boundary conditions

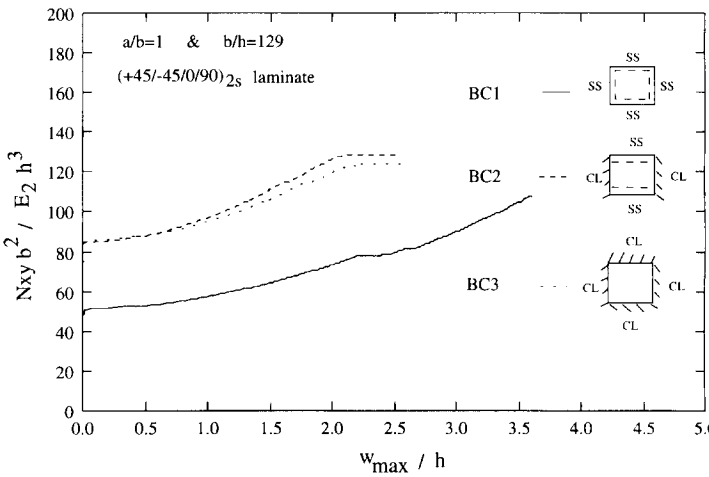

Fig. 16 Progressive failure response of $(\pm 45/0/90)_{2s}$ quasi-isotropic laminate with Hashin criterion for different boundary conditions

Tsai-Wu and the Hashin criteria, respectively. It is observed that the responses for BC2 and BC3 are very close to each other for the Hashin criterion but are quite different for the Tsai-Wu criterion. It is also observed that the progressive failure initiates primarily due to in-plane normal stresses transverse to the fiber direction for all boundary conditions. It is seen that in-plane transverse mode of failure (at the first-ply failure) is followed by in-plane shear mode of failure and transverse shear mode of failure, leading to fiber breakage and delamination in the case of boundary condition BC1. On the other hand, in the case of conditions BC2 and BC3, in-plane transverse mode of failure is followed by transverse shear mode of failure till the onset of delamination. The absolute maximum value of the maximum transverse displacements (w_{max}/h) (obtained for various failure criteria just before the ultimate load) is found to occur in the case of boundary condition BC1 and is equal to 4.2.

Table 5 Comparison of failure loads of $(\pm 45/0/90)_{2s}$ laminate with BC1 boundary condition under negative and positive shear load

Failure criteria	Negative shear			Positive shear		
	First-ply failure load	Ultimate failure load	$(w_{max}/h)^{\oplus}$	First-ply failure load	Ultimate failure load	(w_{max}/h)
Maximum stress	83.05	128.66	2.43	59.38	116.18	1.31
Maximum strain	74.01	75.73	2.03	56.30	87.78	1.16
Tsai-Hill	83.05	126.94	2.43	59.38	116.18	1.31
Tsai-Wu	77.45	125.65	2.19	59.38	116.18	1.31
Hoffman	83.05	125.65	2.43	59.38	116.18	1.31
Hashin	77.45	107.58	2.19	54.21	102.84	1.04

$\oplus$ Non-dimensionalized maximum transverse displacement in the plate at the first-ply failure.

In order to compare failure loads and maximum transverse deflections predicted by various failure criteria under negative shear load with those for positive shear load, failure loads and maximum transverse deflections under negative and positive shear loads for $(\pm 45/0/90)_{2s}$ laminate with BC1 boundary condition are presented in Table 5. It is observed that failure loads under negative shear load are much higher than those for positive shear load irrespective of failure criteria used. However, maximum transverse deflections associated with the first-ply failure load are lower in the case of positive shear than those for negative shear for all failure criteria.

5. Conclusions

It is observed from the study that although failure characteristics are similar to those for the positive shear loading, the numerical values for failure loads and associated maximum transverse displacements are quite different. As concluded by Singh *et al.* (1998), the maximum strain criterion and the Hashin criterion give inconsistent results in comparison to other criteria. The maximum percent difference in first-ply failure loads predicted by various failure criteria occurs for the $(0/90)_{4s}$ laminate as in the case of positive shear. However, the corresponding value for the ultimate failure load occurs for $(\pm 45/0/90)_{2s}$ laminate under negative shear load and for $(0/90)_{4s}$ laminate under positive shear load. Unlike the case of positive shear where maximum difference in failure loads predicted by various failure criteria occurs for the plate with all edges clamped, the maximum percent difference in the first-ply failure loads of $(\pm 45/0/90)_{2s}$) laminate (predicted by various failure criteria) occurs for the boundary condition with all edges clamped whereas the minimum is observed for all edges simply supported and the opposite is true for the ultimate load. Laminates with two parallel edges, or all edges clamped are more susceptible to ultimate failure due to delamination ensuing from the out of plane deflection. The maximum value of the transverse displacement associated with ultimate failure is less than 5 times the plate thickness irrespective of boundary conditions and laminate lay--ups; hence the use of nonlinear theory in the von Karman sense is justified for laminates considered. Overall, this study provides an idea of the reserve strength beyond buckling and upto the first-ply failure and ultimate failure in addition to the progressive failure response. Knowledge of these facts is important from the

considerations of safety design of stronger and lighter composite structural panels.

Acknowledgements

The financial support for this work was made available through a research grant received from the Aeronautics Research Development Board, Ministry of Defence, Government of India.

References

Engelstad, S.P., Reddy, J.N. and Knight, Jr., N.F. (1992), "Postbuckling response and failure prediction of graphite epoxy plates loaded in compression", *AIAA J.*, **30**, 2106-2113.

Hashin, Z. (1980), "Failure criteria for unidirectional fiber composites", *J. Appl. Mech*, **47**, 329-334.

Kosteletos, S. (1992), "Postbuckling response of laminated plates under shear loads", *Composite Structures*, **20**, 137-145.

Lee, H.H. and Hyer, M.W. (1993), "Postbuckling failure of composite plates with holes", *AIAA J.* **31**, 1293-1298.

Reddy, Y.S.N. and Reddy, J.N. (1992), "Linear and non-linear failure analysis of composite laminates with transverse shear", *Composite Science and Technology*, **44**, 227-255.

Singh, S.B., Kumar, A. and Iyengar, N.G.R. (1997), "Progressive failure of symmetrically laminated plates under uni-axial compression", *Structural Engineering and Mechanics*, **5**, 433-450.

Singh, S.B., Kumar, A. and Iyengar, N.G.R. (1998), "Progressive failure of symmetric laminates under in-plane shear: I-Positive shear", *Structural Engineering and Mechanics*, **6**(2), 143-159.

Tsai, S.W. (1986), *Composites Design*, Think Composite, Day-ton, Ohio.

Zhang, Y. and Matthews, F.L. (1984), "Postbuckling behaviour of anisotropic laminated plates under pure shear and shear combined with compressive loading", *AIAA J.*, **22**, 281-286.

Notations

b, h	Width and thickness of the laminate, respectively.
N_{xy}	In-plane shear load per unit length.
E_1	Young's modulus of elasticity in the principal material direction-1 (fiber direction).
E_2	Young's modulus of elasticity in direction transverse to the fiber direction.
E_3	Young's modulus of elasticity in principal material direction-3.
G_{12}, G_{13}, G_{23}	Shear moduli in the planes 1-2, 1-3 and 2-3, respectively.
ν_{12}, ν_{13}, ν_{23}	Major Poisson's ratios in the planes 1-2, 1-3 and 2-3, respectively.
P_f	Average value of first-ply failure loads predicted by failure criteria.
P_u	Average value of ultimate failure loads predicted by failure criteria.
P_c	Buckling load of the laminate.
X_t, X_c	Tensile and compressive strength of lamina in fiber direction, respectively.
Y_t, Y_c	Tensile and compressive strength of lamina in direction transverse to the fiber direction, respectively.
Z_t, Z_c	Tensile and compressive strength of lamina in principal material direction-3, respectively.
R	Shear strength of lamina in plane 2-3.
S	Shear strength of lamina in plane 1-3.
T	Shear strength of lamina in plane 1-2.